Supporting Information

Robinson et al. 10.1073/pnas.1707856115

Methods

All reagents were purchased from Sigma-Aldrich unless stated otherwise.

FcγR Cloning Strategy. FcγR ectodomains (FcγRIIIa-158F, FcγRIIa-131H) were amplified by PCR (see Table S4 for primer sequences) and cloned into pOPINTTG (OPPF) using the In-Fusion system (Clontech Laboratories Inc.) (32, 33).

Alternative allotypes (FcγRIIIa-158V, FcγRIIa-131R) were produced using QuikChange Lightning (Agilent Technologies) following the manufacturer's protocol. Constructs were tested for the expression of secreted protein on a 1-mL scale using transient transfection of HEK293T cells (ATCC) and analysis of the supernatant by anti-His Western blot (Roche), as previously described (34).

Full-length coding sequences encoding FcγRIIa (131R) and FcγRIIIb (NA2) were amplified from cDNA from peripheral blood mononuclear cells from genotyped donors. Full-length coding sequences encoding FcγRIIIa (158F) were amplified from THP-1 cells using cDNA prepared by RT-PCR of total RNA extracted using acid phenol/guanidinium hydrochloride and isopropanol precipitation (35) with SuperScript II reverse transcriptase (Invitrogen) and oligo dT primers (see Table S4 for details of primers used). These sequences were cloned into a plasmid encoding the enzymatic SNAP tag (New England Biolabs) derived from pFB HYG (a gift from J. E. Burns, Leeds Institute of Cancer and Pathology, University of Leeds, United Kingdom.). The plasmids were used to transfect Phoenix A packaging cells (G. P. Nolan, Nolan laboratory, Stanford University, Stanford, CA) so that replication-defective virus particles were produced in the supernatant. These supernatants were filtered and used to infect HEK293 cells. [In the case of FcγRIIIa-expressing cells, virus particles were used to infect cells that had already been infected with a neo resistance vector for stable expression of the common γ-chain of FcεRI gene (*FCER1G*, NM_004106.1). This double transfection was carried out to allow cell-surface expression of FcγRIIIa, which is dependent on the common γ-chain of FcεRI]. Primer sequences for the common γ-chain of FcεRI are shown in Table S4. After 10 d of antibiotic selection, the cells were tested for surface expression using FITC-labeled anti-CD16 mouse monoclonal DJ130c (Dako), which recognizes an epitope in the first extracellular domain. This antibody was also used to show expression of FcγRIIIb. Expression of ectopically expressed FcγRIIa was tested using mouse monoclonal AT10 (CD3204; Caltag Medsystems).

Protein Production and Purification. Receptor ectodomains were secreted from HEK293T adherent cells in roller bottles. Purification was by immobilized metal-affinity chromatography followed by gel-filtration chromatography using a Superdex 200 column. Purified fractions were pooled and concentrated. FcγRIIIa-158F and -158V produced 1–2 mg of culture per liter. To produce protein for cocrystallization, the cells were grown in the presence of the glycosylation inhibitor kifunensine (Toronto Research Chemicals), resulting in ectodomains with glycans of the form $Man_9GlcNAc_2$. To obtain protein with glycans of the form $GlcNAc_1$, the purified protein was treated with Endoglycosidase F1 overnight at 4 °C and then was further purified by gel filtration chromatography to remove the glycosidase and trimmed glycans from the sample. To assess the effect of FcγRIIIa glycosylation on the Affimer protein interaction in SPR, the proteins were produced as above but without kifunensine. A portion of the glycosylated protein was treated with Endoglycosidase F1 as described.

For some experiments, FcγRIIIa ectodomains were biotinylated using EZ-Link NHS-SS-biotin (Thermo Fisher Scientific) according to the manufacturer's instructions. Biotinylation was confirmed using streptavidin-conjugated to HRP to detect the biotin on FcγRIIIa absorbed onto Nunc-Immuno MicroWell MaxiSorp 96-well plates (Thermo Fisher Scientific).

In Vitro Selection of FcγRIIIa-Specific Affimer Protein.

Phage display. We used the libraries described in refs. 6 and 36. We used purified, endoglycosidase F1-treated and biotinylated FcγRIIIa ectodomain (158V) protein as the screening target in phage display. In brief, 5 μL of the phagemid library (10^{12} cfus), was prepanned three times in high-binding-capacity streptavidin-coated wells (Thermo Fisher Scientific) for a total of 1 h. The phage then were incubated with biotinylated FcγRIIIa for 2.5 h. Panning wells were washed 10 times and eluted with 100 μL of 50 mM glycine·HCl (pH 2.2) for 10 min, neutralized with 1 M Tris·HCl (pH 9.1), further eluted with 100 μL of 100 mM triethylamine for 6 min, and neutralized with 50 μL of 1 M Tris·HCl (pH 7). Eluted phage were incubated with exponentially growing ER2738 cells ($OD_{600} = 0.6$) for 1 h at 37 °C and were plated onto lysogeny broth (LB) agar plates. The following day phage were propagated overnight and used in a second panning round displaying FcγRIIIa on streptavidin magnetic beads. Phage and beads were mixed and incubated and then were washed five times using a Kingfisher robotic platform (Thermo Fisher Scientific), eluted, and amplified as above. The final pan was performed using NeutrAvidin high-binding-capacity plates (Thermo Fisher, Scientific) as described above, but the phage were eluted on a vibrating platform for 20 min with 100 μL 100 mM DTT to reduce the disulphide bond of the EZ-Link NHS-SS-biotin before infection of ER2738 cells. Phage were recovered from wells containing FcγRIIIa and control wells to determine the level of amplification in target wells.

Binding specificity by ELISA. Phage ELISA was performed as previously described (6, 36). Streptavidin-coated plates (Thermo Fisher Scientific) were blocked and labeled with 0.4 nM of biotinylated FcγRIIIa for 1 h; then 45 μL of growth medium containing phage propagated from individual clones was added to wells containing biotinylated FcγRIIIa and to wells containing only the biotinylated linker followed by incubation for 1 h and three washings in 300 μL PBS with Tween20 (PBST). Then a 1:1,000 dilution of HRP-conjugated anti-phage antibody (Seramun Diagnostica GmBH) in 100 μL PBST was added for 1 h. Wells were washed 10 times in 300 μL PBST, Affimer protein-mediated phage binding were visualized with 100 μL 3,3′,5,5′-tetramethylbenzidine liquid substrate (Seramun Diagnostica GmBH), and absorbance was measured at 560 nm. Positive binders were submitted for DNA sequence analysis (Beckman Coulter Genomics).

Recloning and modifications. The coding sequences of selected Affimer proteins were PCR amplified, restriction digested with NheI and PstI, and cloned into pET11a containing the similarly digested Affimer proteins scaffold coding region. For biotin labeling Affimer proteins were cloned into a pET11a-scaffold construct encoding a C-terminal cysteine. Individual clones were sequenced to confirm the presence of the correct insert. Plasmids were transformed into BL21 (DE3) cells, and cultures were grown in 400 mL of LB medium to an OD_{600} of 0.6 at 37 °C before the addition of isopropyl β-D-1-thiogalactopyranoside to a concentration of 1 mM. After a further 6 h, cells were harvested,

resuspended in 25 mL of 1× BugBuster (Novagen) with benzonase, mixed for 20 min, and then heated to 50 °C for 20 min. The cleared supernatant was mixed with 500 μL Ni-NTA resin (Expedeon) for 1 h, washed three times in 30 mL wash buffer (50 mM PBS, 500 mM NaCl, 20 mM imidazole, pH 7.4), and eluted in 1 mL of elution buffer (50 mM PBS, 500 mM NaCl, 300 mM imidazole, pH 7.4).

Confirmation of FcγRIIIa binding. Freshly purified Affimer proteins proteins were used in SPR assays to confirm binding to both common FcγRIIIa allotypes (158F and V). SPR was carried out on a BIAcore T200 biosensor (GE Healthcare). Soluble FcγRIIIa ectodomains of the 158V allotype were immobilized (100 RU) in 10 mM acetate (pH 5.0) on a CM5 sensor chip (GE Healthcare) using amine coupling, as directed by the manufacturer. Affimer proteins were used as analytes in single-cycle kinetics with 2-min injections of increasing concentrations from 123 nM to 10 μM at a flow rate of 30 μL/min in HBS-EP+ (GE Healthcare) running buffer. The FcγRIIIa surface was regenerated between cycles using a 60-s injection of 10 mM glycine (pH 2.0) at 30 μL/min.

A blank amine-coupled flow cell was used as reference, and zero-concentration controls were used in double referencing. All analysis was carried out using BIAcore T200 Evaluation Software v1.0. Langmuir 1:1 kinetic models were fitted to reference-subtracted sensorgrams, and steady-state affinity models were fitted.

For ITC, protein samples were dialyzed against PBS overnight at 4 °C, and this buffer was used for control titrations. ITC was performed using a MicroCal iTC200 instrument (Malvern Instruments) at 25 °C. An initial injection of 0.5 μL over 1 s was followed by 19 injections of 2 μL, each over 4 s with 2 min spacing, while stirring at 750 rpm and with a reference power of 5 μCal/s. The sample cell contained 10 μM FcγRIIIa-158V, and Affimer protein was injected at a concentration of 100 μM. Results were analyzed using Origin software after subtraction of a control titration of Affimer protein into buffer.

Cell-Based IgG-Binding Assays. Constructs encoding FcγRIIa (27Q 131H), FcγRIIIa (158F and V), and FcγRIIIb-NA2 were stably transfected into HEK293 cells and used to investigate FcγRIIIa-specific inhibition of IgG1 HAG binding. Cells were harvested with trypsin and EDTA and then were resuspended at 250 cells/μL in DMEM (Invitrogen) containing 10% FCS. Each selected Affimer protein was added at 50 μg/mL and was incubated at room temperature for 1 h. The cells were cooled on ice and incubated with 100 μg/mL HAG (The Binding Site) for a further 2 h. The cells were incubated on ice for 1 h with 100× diluted goat anti-human κ light-chain $F(ab')_2$ fragments labeled with PE (AbD Serotec; Bio-Rad). Cells were washed in ice-cold FACS buffer (PBS with 2% FCS and 2 mM EDTA) and then were fixed in 2% formaldehyde to prevent loss or phagocytosis of complexes. Binding of HAG to the FcγR-expressing cells was assessed using a Guava easyCyte Flow Cytometer (Millipore) using empty vector-transfected cells as controls.

The median fluorescence intensity was determined for each tube, and averages of triplicate values were determined for each cell line. Statistical significance was calculated by using two-tailed Student's *t* tests for inhibition of HAG binding and an assumption of unequal variance.

Blockade of Effector Functions in the THP-1 Macrophage Cell Line.

Characterization of FcγR expression on THP-1 cells under different culture conditions. To select suitable monoclonal antibodies for these studies, we undertook some genetic and transcriptional analyses of the THP-1 cell line. The extracellular domains of the CD32 receptors (FcγRIIa, FcγRIIb, and FcγRIIc) are almost identical, and consequently not all CD32 mAbs are able to fully distinguish between the FcγRII subtypes. CD32-IV3 (STEMCELL Technologies) has been reported to recognize only FcγRIIa (37, 38), whereas CD32 3D3 (BD Pharmingen) recognizes FcγRIIa-131R, FcγRIIb, and FcγRIIc. The THP-1 cell line was therefore genotyped for *FCGR2A*-131H/R by direct sequencing of genomic DNA using published assays (39). The *FCGR2C* STP/ORF variant and transcription of specific *FCGR2B/C* isoforms were determined as described in ref. 40.

Human monocytic THP-1 cells (European Collection of Cell Cultures) were grown in RPMI 1640 medium containing 10% FCS and 2 mM L-glutamine at 37 °C in 5% CO_2. The level of FcγR cell-surface expression was initially determined in resting and PMA-differentiated THP-1 cells. Briefly, THP-1 cells were seeded at a density of 2×10^5 cells/mL and were incubated with medium alone or with 50 ng/mL PMA for 18 h at 37 °C. The medium containing PMA was removed, and the cells were rested for 48 h in the presence of medium alone.

The level of expression of cell-surface markers (FcγRIII: CD16-3G8, Caltag-Medsystems; CD32-IV.3, STEMCELL Technologies) and CD32-3D3, BD Pharmingen; CD64-10.1, Beckman Coulter Immunotech) and the percentage of cells positive for these markers were evaluated in differentiated THP-1 cells incubated for an additional 24 h in the presence of medium alone or after stimulation with 250 ng/mL LPS. Cells harvested using trypsin and EDTA were washed in PBS–BSA, stained with directly conjugated antibodies (diluted 250× for 30 min at 4 °C, in the dark), washed with PBS–BSA, resuspended in PBS–BSA, and analyzed by flow cytometry (Becton Dickinson LSRII).

TNF production. TNF production was assessed in differentiated THP-1 cells (2×10^5 cells in 500 μL) that were incubated for 1 h at 37 °C in medium alone (negative control) or with 250 ng/mL LPS (positive control) or with 100 μg/mL HAG before the addition of 10 μg/mL Brefeldin A (an intracellular protein transport inhibitor) and further incubation for 3 h at 37 °C in 5% CO_2. Blocking antibodies were obtained from Ancell Corporation. The antibody clones were 3G8 for CD16 (a known blocking antibody), 7.3 for CD32, and 10.1 for CD64. Cells were washed in PBS with 2% BSA, fixed in 2% paraformaldehyde for 30 min, washed again, and then permeabilized using 0.3% saponin in PBS–BSA (15 min at room temperature). Anti–TNF- PE or IgG1-PE (Serotec) diluted 1:500 in PBS–BSA + 0.1% saponin was added for 30 min at room temperature in the dark. Cells were washed and resuspended in PBS–BSA for immediate analysis by flow cytometry (Becton Dickinson LSRII).

***Phagocytosis of IgG-opsonized* E. coli.** Phagocytosis was assessed by the incubation of untreated or PMA-differentiated THP-1 with 10 μg/mL green fluorescent *E. coli* (Thermo Fisher). The *E. coli* were either untreated or preopsonized with 5% human AB serum [complement inactivated at 56 °C for 30 min]. *E.coli* were washed in PBS to remove excess serum, pelleted at 1,600 × *g* for 15 min, then added to the THP-1 cells and incubated for 1 h at 37 °C or in cells precooled to 4 °C (negative control). Cells were washed in PBS–BSA, stained with 0.4% Trypan blue to quench extracellular fluorescence, washed three times with PBS–BSA, resuspended in PBS–BSA, and analyzed by cytometry using a Becton Dickinson LSRII flow cytometer.

Crystallization and Structure Solution. Endoglycosidase F1-treated FcγRIIIa crystals 20–30 μm in size were grown in 200-nL drops (100 nL FcγRIIIa ectodomain + 100 nL precipitant) in 96-well plates using noncontact dispensing robotics (MicroSys; Cartesian). Crystallization trials used the method of Walter et al. (41) at 8.9 mg/mL for 158F and at 11.4 mg/mL for 158V. Cocrystallization of FcγRIIIa with Affimer proteins was performed by mixing in a 1:1 molar ratio and incubation at room temperature for 30 min before setting up crystallization trials. Conditions are shown in Table S5.

Crystals were detected in a number of conditions with data being collected from condition 41 or 43 of the Hampton PEG/Ion screen [20% (wt/vol) PEG 3350, 0.200 M potassium di-hydrogen phosphate, and 20% (wt/vol) PEG 3350, 0.200 M ammonium phosphate monobasic] or optimizations around these conditions (41).

For diffraction data collection, crystals were loop mounted and cryo-cooled in liquid nitrogen. Data were collected at Beamline I24, Diamond Light Source, with the X-ray beam defocused to 20×20 μm^2 from multiple positions on each crystal. All diffraction data were integrated using XDS (42) and scaled using AIMLESS (43). Phases were obtained via molecular replacement using PHASER (44). A subsection of a complex of an Affimer protein bound to a soluble protein was used as a search model. Refinement was carried out using PHENIX (45). Ligands and sugar modifications were built manually into Fo-Fc maps using COOT (46). In the case of AfG3 additional noncrystallographic symmetry torsion restraints were applied during refinement. The quality of the protein structure was assessed using MolProbity (47). Data collection and refinement statistics are given in Table 1.

The residues involved in Affimer protein binding to FcγRIIIa were identified based on the Protein Interaction Calculator (48) and visual inspection.

MD Simulations. MD simulations were prepared with the AmberTools 14 suite of programs and performed with AMBER14 (49), ff14SB47 (50), and GLYCAM_06j-1 (51). Simulations used 128 processors of the MARC1 supercomputer, Advanced Research Computing, University of Leeds, United Kingdom. To simulate Affimer protein–FcγR interactions in water, models were first generated of each Affimer protein in complex with either FcγRIIIa (-158F allotype for AfG3 and -158V allotype for AfF4) or FcγRIIIb-NA2. The FcγRIIIb-containing complex was generated by mutation of the FcγRIIIa–Affimer protein crystal structures to resemble the FcγRIIIb-NA2 structure through the use of TRITON/MODELER (52).

After mutagenesis, the xleap program of AmberTools 14 was used to add hydrogen atoms, form disulphide bridges, and add β1,4-linked GlcNAc residues at glycosylation sites in FcγRIIIa/FcγRIIIb. Complexes were then placed in a TIP3P water box with a 10.0-Å cutoff, and the system was neutralized with Na^+ ions. The system was equilibrated through an initial energy minimization, which was followed by 80 ps of restrained MD during which the system was heated to 300 K with gradual releasing of restraints. An unrestrained MD simulation of 200 ns was then performed. For each complex, simulations were repeated in triplicate.

Calculations of the rmsd showed that all simulations remained stable and that 200 ns was sufficient for the rmsd to converge to a stable value, indicating that no significant global conformational changes were taking place over MD timescales.

Trajectories were analyzed with the cpptraj module of AMBER14, which was used to calculate inter- and intramolecular H-bonds, per residue atomic fluctuations and interatomic distances. H-bonds with a cutoff of 3.2- Å and 160°, which were present for more than 5% of the total trajectory, were recorded. VMD (53) was used to render videos of the simulations, and PyMOL was used to generate representative figures (54).

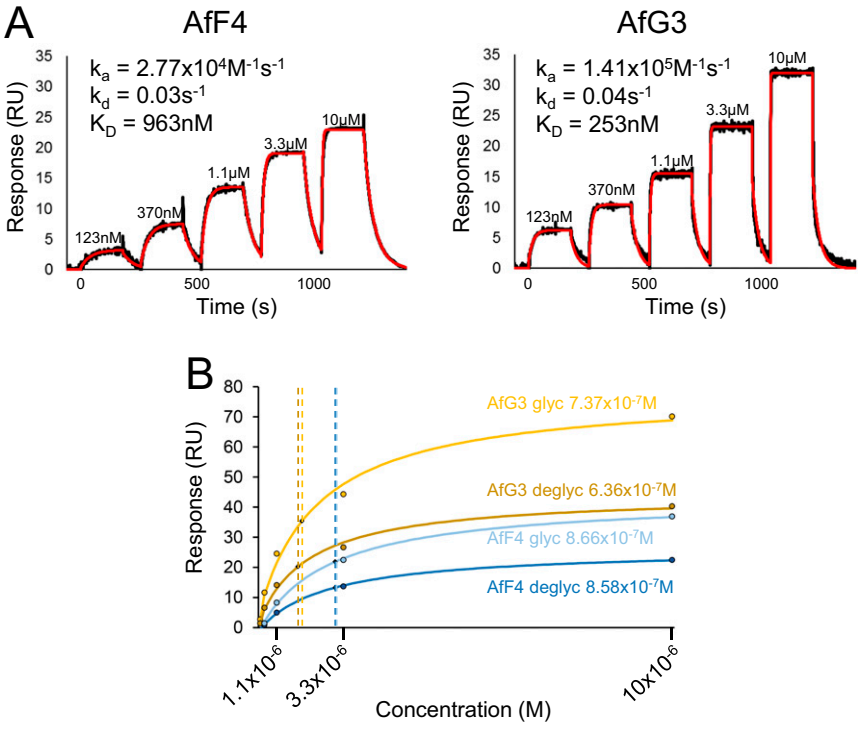

Fig. S1. FcγRIIIa interactions with AfF4 and AfG3 (123nM-10μM) by surface plasmon resonance. (*A*) Amine coupled receptors. A single cycle kinetics 1:1 binding model (superimposed red line) provided kinetic measurements of association (k_a) and dissociation (k_d) and equilibrium dissociation constant (K_D) as indicated. Interaction kinetics exceeded the measurement capabilities of the instrument at higher Affimer protein concentrations. (*B*) Orientated C-terminal Avitag-immobilized receptors. Steady-state affinity measurements from SPR for each Affimer protein interaction with immobilized fully glycosylated and Endo F1-treated FcγRIIIa.

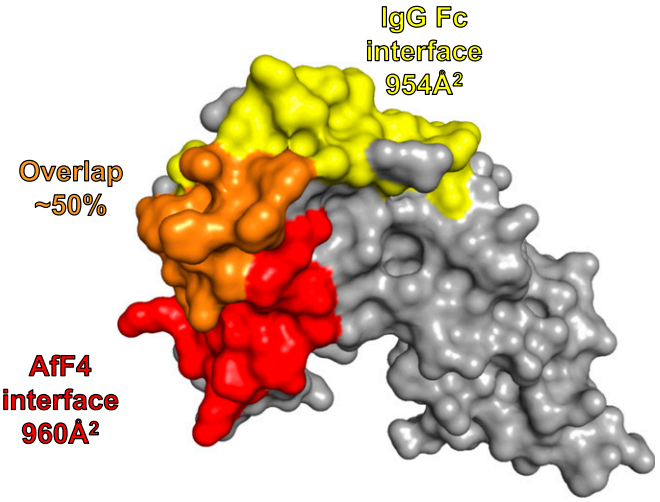

Fig. S2. Overlapping binding sites on FcγRIIIa for IgG Fc and AfF4. FcγRIIIa-IgG Fc from 3SGJ (yellow) and -AfF4 from 5ML9 (red) interfaces overlap by ~50% (orange) illustrating the steric nature of the IgG inhibition. Interface surface areas were calculated using PISA (EMBL-EBI).

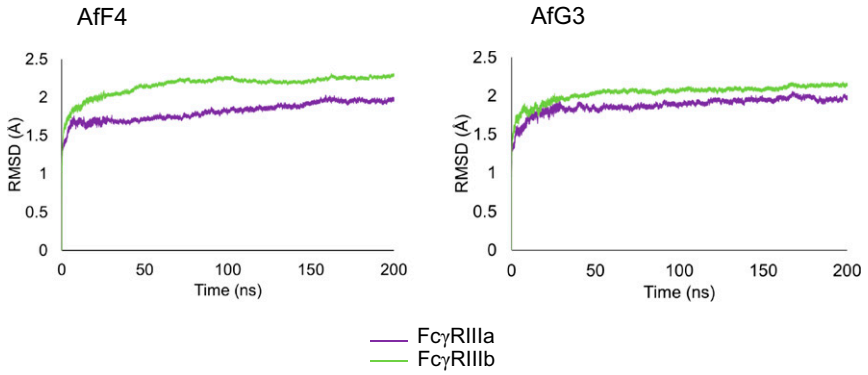

Fig. S3. Per-residue root mean square deviation (RMSD) analysis of FcγRIIIa/b-AfF4 and -AfG3 molecular dynamics trajectories. RMSD values were averaged over three repeats and show that all simulations remained stable during the timescale of the simulations, and that 200 ns was sufficient for the RMSD to converge to a stable value.

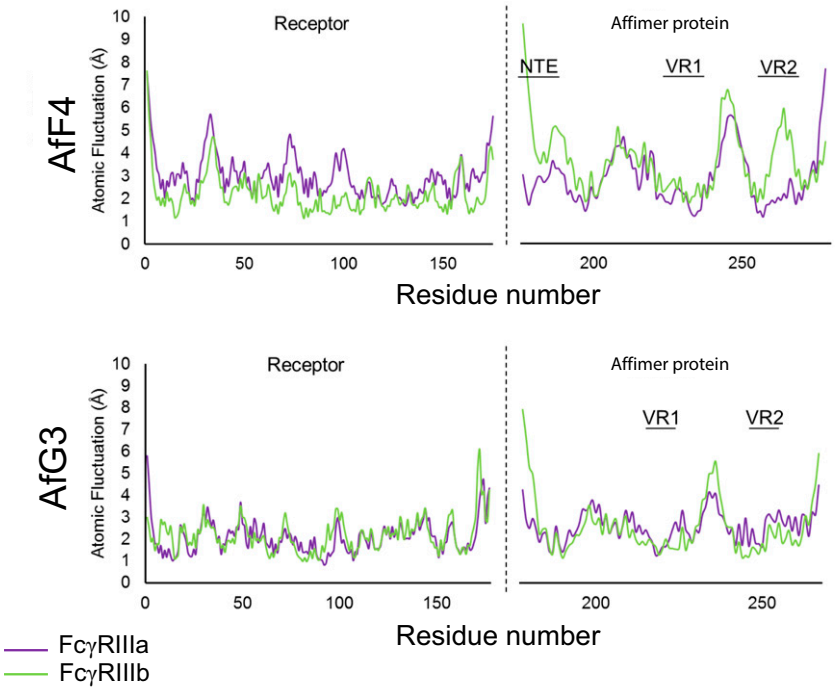

Fig. S4. Atomic fluctuation by residue of FcγRIIIa/b-AfF4 and –AfG3 molecular dynamics trajectories. Higher values represent greater fluctuation. All values were averaged over three repeats. Purple plots represent FcγRIIIa-containing simulations and green plots represent FcγRIIIb-containing simulations.

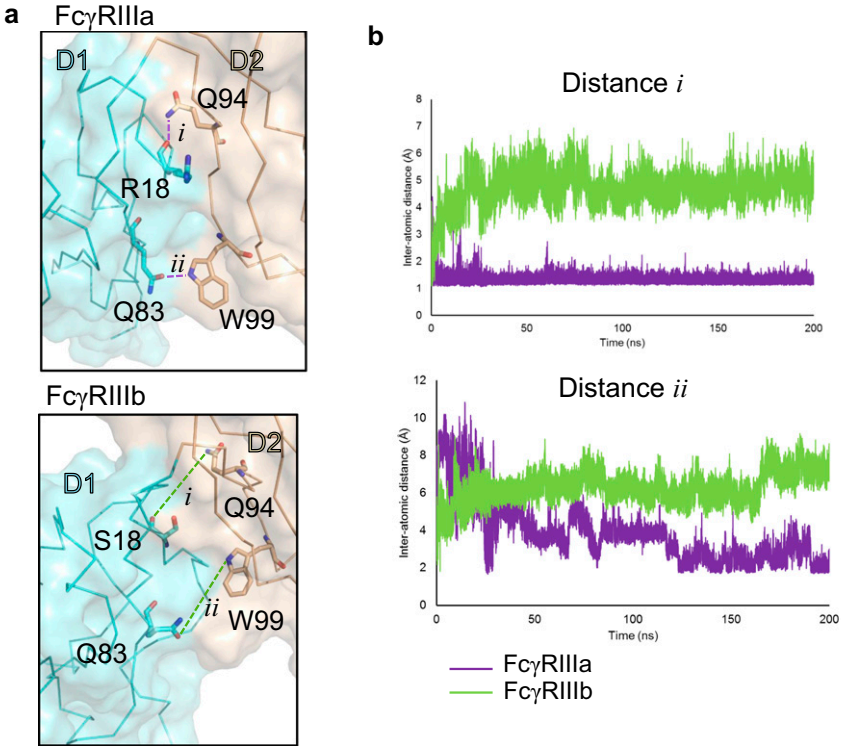

Fig. S5. Molecular dynamics simulations suggest a proposed mechanism of AfG3-mediated FcγRIIIa inter-domain angle restriction. (*A*) View of D1–D2 interdomain hinge in FcγRIIIa and FcγRIIIb after 200 ns of molecular dynamics simulation. D1 depicted in aquamarine, D2 depicted in wheat. (*B*) Measurements *i* and *ii* describe interatomic distances over the course of the 200 ns AfG3 simulations for both FcγRIIIa (purple lines) and FcγRIIIb (green lines) averaged over three repeats. Formation of the γaArg18-γaGln94 H-bond early in the simulations leads to formation of an additional interdomain H-bond between γaGln83 and γaTrp99. In FcγRIIIb the lack of *i* formation leads to greater flexibility between D1 and D2 preventing the formation of *ii*.

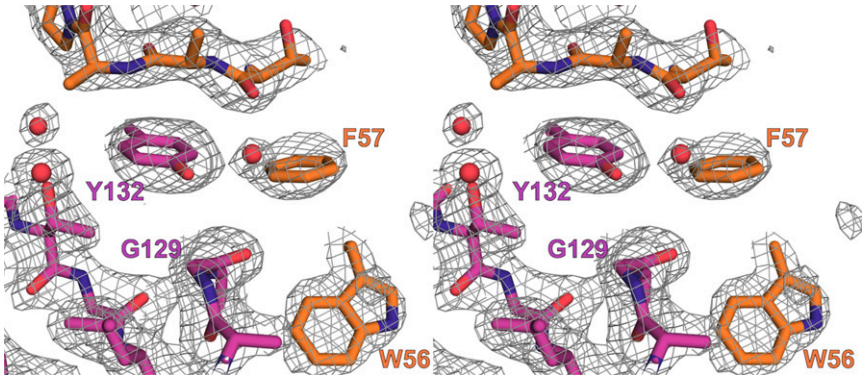

Fig. S6. Stereoimage of an AfF4-FcγRIIIa ectodomain model fitted to electron density map contoured at 2.0 sigma. FcγRIIIa in purple stick and AfF4 in orange stick representation.

Table S1. Specific AfF4 interactions at the Affimer proteins–protein interface seen in crystal structure 5ML9

FcγRIIIa						Affimer proteins F4		
Position	Amino acid	Atom	Distance, Å	Water	Distance, Å	Position	Amino acid	Atom
125	Gln	[Oε1]	2.7	–	–	55	His	[Nε2]
130	Arg	[O]	2.9	–	–	57	Phe	[N]
130	Arg	[Nε]	2.5	–	–	55	His	[O]
130	Arg	[Nε2]	3.1	415	2.9	54	Glu	[O]
131	Lys	[Nω2]	2.7	–	–	58	Pro	[O]
131	Lys	[Nω2]	2.7	–	–	60	Thr	[Oγ1]
132	Tyr	[N]	2.8	–	–	85	Asn	[Nδ2]
132	Tyr	[N]	2.8	403	2.6	85	Asn	[N]
134	His	[N]	2.4	–	–	19	Glu	[Oε2]
134	His	[Nε2]	2.7	–	–	22	Glu	[Oε2]
135	His	[N]	3.1	–	–	19	Glu	[Oε2]
135	His	[Nε2]	2.5	–	–	22	Glu	[Oε2]
136	Asn	[O]	2.5	314	2.6	19	Glu	[N]
137	Ser	[Oγ]	3.1	–	–	16	Asn	[Nδ2]
137	Ser	[Oγ]	2.8	407	2.9	16	Asn	[Nδ2]
138	Asp	[N]	2.6	–	–	16	Asn	[Oδ1]
–	–	–	–	407	2.9	62	Thr	[Oγ1]
–	–	–	–	407	2.7	49	Glu	[Oε2]

Table S2. Average B factor per chain of AfG3

Chain	Average B value
A	66.1
B	104.2
C	73.6
D	76.5
Water	62.8
All	80.1

Table S3. Specific interactions at the AfG3–FcγRIIIa interface seen in crystal structure 5MN2

FcγRIIIa						Affimer proteins G3		
Position	Amino acid	Atom	Distance in Å	Water	Distance in Å	Position	Amino acid	Atom
17	Tyr	[OH]	2.8	520	2.7	85	His	[O]
83	Gln	[Nε2]	2.7	–	–	83	Gln	[O]
83	Gln	[Oε1]	2.6	517	2.9	83	Gln	[N]
85	Glu	[Oε2]	2.8	–	–	85	His	[N]
85	Glu	[Oε2]	2.6	520	–	–	–	–
86	Val	[N]	3.2	615	3.0	85	His	[Nε2]
99	Val	[N]	3.2	–	–	51	Gly	[O]
167	Thr	[Oγ1]	3.4	–	–	86	Asn	[Nδ2]
169	Asn	[N]	3.1	–	–	83	Gln	[Oε1]
169	Asn	[O]	2.9	–	–	83	Gln	[Nε2]
–	–	–	–	517	2.9	83	Gln	[O]
–	–	–	–	517	2.8	52	Phe	[O]
98	Trp	[Nε]	3.0	517	–	–	–	–
86	Val	[O]	3.0	615	–	–	–	–

Table S4. Selected H-bond distances in the key interactions between FcγRIIIa/b and AfG3 in MD simulations

		FcγRIIIa–AfG3			FcγRIIIb NA2-AfG3		
Donor residue	Acceptor residue	Occupancy, %	Average distance, Å	Average angle, °	Fraction of simulation	Average distance	Average angle
Intermolecular H-bonds							
γa/b-Trp98 [N]	AfG3-Gly51 [O]	26.14	2.91	159.11	15.92	2.85	151.78
γa/b-Val99 [N]	AfG3-Gly51 [O]	44.22	2.89	161.24			
γa/b-Arg18 [NH1/NH2]	AfG3-Asn86 [OD1]	39.30	2.84	152.25			
Intramolecular H-bonds							
γa/b-Gln94 [NE2]	γa/b-Arg/Ser18 [O]	69.53	2.85	162.62	26.38	2.76	157.72
γa/b-Glu21 [H]	γa/b-Arg/Ser18 [O]				37.44	2.88	154.16
γa/b-Leu20 [H]	γa/b-Arg/Ser18 [O]				57.48	2.85	159.65
γa/b-Arg/Ser18 [H]	γa/b-Ala95 [O]	32.87	2.87	151.96			
γa/b-Arg18 [NH1/NH2]	γa/b-Glu166 [OE2]	35.71	2.81	151.90			
γa/b-Arg18 [NH1/NH2]	γa/b-Glu166 [OE1]	19.15	2.81	151.57			
γa/b-Trp98 [HE2]	γa/b-Gln83 [OE1]	38.31	2.84	156.71			

Table S5. Protein/Affimer protein crystallization conditions

Protein	Affimer protein	Screen	Condition
FcγRIIIa 158F	AfG3	JCGS$^+$ (D12)	20.0% (vol/vol) glycerol 16.0% (wt/vol) polyethylene glycol 8000 0.04 M potassium di-hydrogen phosphate
FcγRIIIa 158V	AfF4	JCSG$^+$ (E2)	2.0 M ammonium sulfate 0.1 M sodium cacodylate (pH 6.50) 0.2 M sodium chloride

Table S6. Sugar-modified residues

FcγRIIIa–AfG3	FcγRIIIa–AfF4
A Asn38	A Asn45
A Asn45	A Asn74
A Asn74	A Asn169
A Asn162	
A Asn169	
B Asn45	
B Asn74	

Table S7. Cloning primer sequences

Primer name	Vector/fragment	Size, bp	Sequence (5′–3′)
FCGR2A ectoF	pOPINTTG 2Aectodomain	551	GCGTAGCTGAAACCGGCGCTCCCCCAAAGGCTGTGC
FCGR2A ectoR			GTGATGGTGATGTTTGCTGGGCACTTGGACAGTGATGG
FCGR2A SDMF	pOPINTTG 2Aectodomain 131R	551	TCCCAGAAATTCTCCCGTTTGGATCCCACCTTC
FCGR2A SDMR			GAAGGTGGGATCCAAACGGGATTTCTGGGA
FCGR3A ectoF	pOPINTTG 3A ectodomain	551	GCGTAGCTGAAACCGGCGAAGATCTCCCAAAGGCTGTGGTG
FCGR3A ectoR			GTGATGGTGATGTTTACCTTGAGTGATGGTGATGTTCACAG
pFBHYGFCGR2AF	pFBHYGSNAP 2A full length	986	AATTGTCGACGAATTCATGACTATGGAGACCCAAATGTC
FCGR2A SNAPR			CTTTGTCCATGGATCCGTTATTACTGTTGACATGGTC
pFBHYGFCGR3AF	pFBHYGSNAP 3A full length	905	AATTGTCGACGAATTCATGGGTGGAGGGGCTGGGGAA
FCGR3A SNAPR			CTTTGTCCATGGATCCTTTGTCAGGGTCTTTTCTCCA
FCGR3ASDMf	pFBHYGSNAP 3A full-length 158V	905	CTTCTGCAGGGGGCTCTTGTTGGGAGTAAAAATGT
FCGR3ASDMr			ACATTTTTACTCCCAACAAGCCCCCTGCAGAAG
pFBHYGFCGR3AF	pFBHYG 3B full length	842	AATTGTCGACGAATTCATGGGTGGAGGGGCTGGGGAA
FCGR3B R			GCCGCTCGAGGATCCTCAAATGTTTGTCTTCACAGAG